communications materials

Article

https://doi.org/10.1038/s43246-024-00723-w

Automated chain architecture screening for discovery of block copolymer assembly with graph enhanced self-consistent field theory

Check for updates

Yuchen Zhang, Weiling Huang & Yi-Xin Liu ✉

The diverse chain architectures of block copolymers makes them important for exploring new self-assembly, but poses significant challenges for identifying the stability windows of desired mesophases within the vast parameter space. Here, we present an automated workflow for screening chain architectures to discover new self-assembly. Utilizing graph-enhanced self-consistent field theory complemented by a scattering-based identification strategy, our approach enables the automated computation of arbitrary chain architectures and their phase behavior. This framework successfully identifies stable windows for a novel PtS phase in AB-type block copolymer melts, with two distinct chain architectures emerging from the screening process. Our findings demonstrate the utility of this method in stabilizing desired self-assembly and exploring new mesophases. The flexibility of our approach allows for straightforward extension to multi-species and multi-component systems and further integration with metaheuristic optimization techniques to enhance its potential for materials design.

Crystal structures formed by hard matters including atoms, ions and small molecules have historically been extremely desirable materials due to their spatial periodicity and diverse symmetries[1]. In contrast to the limited choice of building blocks dictated by the periodic table of elements on the atomic scale, the substantial tunability of soft matters on the mesoscale enables a structural variety believed to far surpasses that of atomic compounds[2–4]. An increasing number of mesoscopic crystals, possessing geometrical structures analogous to hard atomic crystals[5,6], as well as those seemingly exclusive to the mesoscale[7–9], have been investigated through both experiments and simulations over recent decades[10–12]. The remarkable potential of mesoscopic metallurgy is driven by the self-assembly of soft materials, such as nanoparticles[13,14], colloids[11,15,16] and macromolecules[17–19]. Among these soft building blocks, block copolymers (BCPs) have attracted considerable attention due to their rich phase behavior[10,17], highly modifiable chain architectures[18,19] and easily adjustable system compositions[20,21]. In particular, the ongoing enrichment of the types of ordered phases in AB-type block copolymers has continuously positioned them as a hotspot for the exploration of new mesophases[22–25].

By varying the two major parameters of the simplest AB diblock copolymer melts, the Flory-Huggins interacting parameter, χ, and the volume fraction of species A, f_A, stability of various mesophases including lamellae (LAM), hexagonal packed cylinders (HEX), body-centered cubic (BCC), face-centered cubic (FCC), hexagonal close-packed (HCP)[26], double gyroid (DG)[7,27,28], hexagonally perforated lamellar (HPL)[29,30], and O^{70}[31] have been studied extensively both in experiments and in theory[12]. By introducing miktoarm architectures, two more ordered phases, σ[22] and A15[9,18] phases, are found to be stable. Mutating single-block arms to linear multi-block arms in star block copolymers further stabilizes several nonclassical phases, such as graphene-like cylinders (C_3)[23] and square array of cylinders (C_4)[23,32]. Recently, asymmetric branching in chain architectures leads to stability windows for low-coordination number (CN) spherical phases, such as simple cubic (SC), hexagonally packed spheres with aligned layers (iHP^a) and cubic diamond (DS_C)[24]. Stability of the single gyroid (SG) phase is achieved in highly asymmetric linear BABAB pentablock copolymers[25]. Since the number of ordered phases found in AB-type block copolymers is relatively small as compared to 230 space groups, the chance to find new stable phases is still sizable[4]. However, conventional approaches[19,33] that start from manually designed polymer architectures impose limitations on the possible phase behavior and appear inefficient as compared to the rapidly expanding scope of ordered phases.

Department of Macromolecular Science, State Key Laboratory of Molecular Engineering of Polymers, Fudan University, Shanghai, China.
✉e-mail: lyx@fudan.edu.cn

In this letter, we explore the phase behavior of block copolymers from a different perspective and automate the discovery of new specific stable phases in a wider and more flexible search space by incorporating polymer architectures into the parameter space. By not requiring a priori specification of a polymer system, this approach manages to bypass the limitations imposed by human bias. It attempts to uncover the intrinsic relationship between polymer architectures and phase behavior by allowing the target phase itself to reveal the appropriate architectures, rather than imposing one that is deemed tractable from a human perspective. It is expected that, utilizing the power of modern computing to test many more architectures than human intuition alone could sort through, the polymer architectures capable of stabilizing the target phase will eventually be discovered. To better demonstrate the impact of variable chain architectures on phase behavior, we continue to explore new stable phases within the well-explored AB-type block copolymer system which seems to be exhausted and poses a significant challenge to find one more new stable ordered phase.

We propose a fully automated workflow aiming at discovering new phases, which enables the massively parallel screening of randomly generated polymer architectures based on the mean-field free energy comparisons with metastable phases. The workflow is made possible by a brand new computing framework for self-consistent field theory (SCFT) calculations which combines the power of several high level techniques. Firstly, we propose a generic graph representation, enabling online switching architectures during the automated run without re-implementing SCFT algorithms. This representation also facilitates automatic random phase approximation (RPA) calculations for arbitrary non-cyclic architectures to obtain approximate order-disorder transitions (ODT), delineating ordered phase regions for the reference of future calculations. Secondly, we employ our previous developed scattering-based automated identification strategy (SAIS)[34] to ensure precise computation of the free energies for candidate phases. Our target phase for demonstration is the PtS phase that crystallizes in the tetragonal crystal system. This represents a low coordination number spherical phase, where the arrangement of Pt and S atoms is similar to that in the iHP[a][35]. After the automated screening of more than 6000 randomly generated architectures, we successfully identify two polymer architectures exhibiting notable stable region for the PtS phase, which predicts PtS as a new stable phase in AB-type block copolymers.

Results

Graph representation of block copolymers

Our workflow begins with the graph representation of arbitrary non-cyclic molecules, providing a convenient interface for the generation and analysis of block copolymer architectures. This representation automates the analysis of the input architecture to determine the required propagator sequence, allowing existing SCFT algorithms to proceed seamlessly without requiring manual reconfiguration whenever the architecture changes. First of all, a chain architecture is represented as a simple graph $G = (V, E)$ comprises a set of vertices $V = \{1, 2, \ldots n_v\}$ equipped with an edge relation $E \rightarrow \{\{u, v\}|u, v \in V\}$, defined as a binary relation over V that is both symmetric ($E(u, v)$ whenever $E(v, u)$ for all vertices $u, v \in V$) and irreflexive ($E(v, v)$ for no vertices $v \in V$)[36,37]. We establish bijective mappings between edges and vertices of the graph and blocks and joints of the block copolymer, respectively. The incidence function $M(u, v)$ maps the properties of each block, including species (A or B), length (f), discrete size of the chain contour (Δs), etc., onto each edge. Vertices with a degree of 1 are denoted as leaf vertices, and other vertices are joint vertices. The process of constructing a graph from a block copolymer is illustrated in Fig. 1(a) and (b).

To automatically analyze the given architecture, we first employ a depth-first algorithm[38,39] to traverse from all the leaf vertices to an arbitrary chosen goal vertex. Then, we employ topological sort[39] to specify the computation sequence for all propagators. The solution of forward propagators (from leaf vertices to the goal vertex), $\{q_{uv}\}$ and backward propagators (from the goal vertex to every leaf vertex), $\{q^{\dagger}_{uv}\}$, involves gathering all the depth-first paths, as illustrated in Fig. 1c. Here u, v represent the starting and ending vertices of the propagator, respectively. Forward propagators $\{q_{uv}\}$ constitute an ordered pair of vertices, $A_F \rightarrow \{\{u, v\}|u, v \in V\}$, called arcs, defined as a binary relation over V that is both asymmetric and irreflexive. A simple directed graph is represented as $G_F = (V, A_F)$, comprises a set of vertices $V = \{1, 2, \ldots n_v\}$ and a set of arcs A_F. Similarly, $G_B = (V, A_B)$ is a graph formed by the backward propagators $\{q^{\dagger}_{uv}\}$. As all propagators originating from joint vertices require initialization by all other propagators connecting to their starting vertices, they exhibit interdependence, necessitating the automatic specification of their computation sequence to ensure that for every arc $A(u, v)$ in the directed graph, u is visited only after all its dependencies are visited. The solution of a propagator can only begin after all propagators in its dependency list has been computed.

To achieve this, we employ topological sort to traverse the directed graphs. All propagators originating from leaf vertices will be sorted first, for example, q_{12}, q_{43}, q_{56}, q_{76}, as depicted in Fig. 1d. This satisfies the dependency lists for q_{32} and q_{62}, completing the computation of all forward propagators. Next, utilizing forward propagators, $q^{\dagger}_{21}, q^{\dagger}_{23}, q^{\dagger}_{26}$ can be solved, which further satisfies the requirements for $q^{\dagger}_{34}, q^{\dagger}_{65}, q^{\dagger}_{67}$, completing the computation sequence for all propagators. Through the above analysis, the input architecture is transformed into a graph representation, and the modified diffusion equations (MDEs) for solving each propagator are fully specified. Other details of the formulation of SCFT and its implementation can be found in Supplementary Note S1.

Random architecture strategy

To ensure the automated SCFT computations of arbitrary architectures proceed within the ordered phase region, we employ RPA[40–42] to obtain the approximate ODT. The form factor $P(\mathbf{k}) = \sum_{m,n} g_{mn}(\mathbf{k})$ is crucial for obtaining the scattering matrix and structure factor, where $\mathbf{k}$ is the scattering vector and m, n iterates all the edges[41,42]. To achieve automated calculation of $P(\mathbf{k})$, we utilize the A* algorithm[43] to find the shortest path connecting any pair of edges (m, n), thereby avoiding manual analysis and path selection for any architecture. Then, we leverage well-established optimization methods and root-finding algorithms to determine approximate $(\chi N)^*$ for ordered phases. The detailed calculation process can be found in Supplementary Note S2.

To avoid possible limitations imposed by manual design, each architecture is formed by randomly combining a number of blocks. The distribution of species (A or B) and lengths (volume fractions) among blocks are randomly assigned. Through this approach, we can obtain an ensemble of AB-type block copolymers encompassing tree-like, linear, and star architectures simultaneously. The detailed process of architecture generation can be found in Supplementary Note S3.

To ensure every SCFT calculation converged to its initial given phase without human supervision, we utilize our previously developed SAIS[34] to identify the results. This strategy computes reflections of ordered phases output by the SCFT and compare them with known ordered phases. As SCFT initialized with given structure may converge to other structures, SAIS ensures the computed free energy belongs to our target structure by repeating the SCFT calculation until the target structure is identified. We considered a wide range of ordered phases as candidates, and include their scattering patterns in Supplementary Note S4.

Automated exploration of target phases

Once the entire process of architecture screening, from random generation to identification for free energy comparison, has been completed, it is time to proceed with the automated exploration for a target phase. Recent studies revealed the stability of some low-CN spherical and cylindrical phases in neat AB-type block copolymer melts[23,24]. To demonstrate the validity of our method, we choose PtS from inorganic crystals as the target phase which has not been found stable in AB-type block copolymers before this work. PtS is a low-CN spherical phase (CN = 4) with a similar packing mode of spherical domains compared to the hexagonally packed spheres with aligned layers (iHP[a])[35]. The lattice sites originally occupied by Pt and S atoms are replaced by uniform spherical domains of species A, as demonstrated in Fig. 2. Based on the characteristics of such ordered phases, we set the total number of

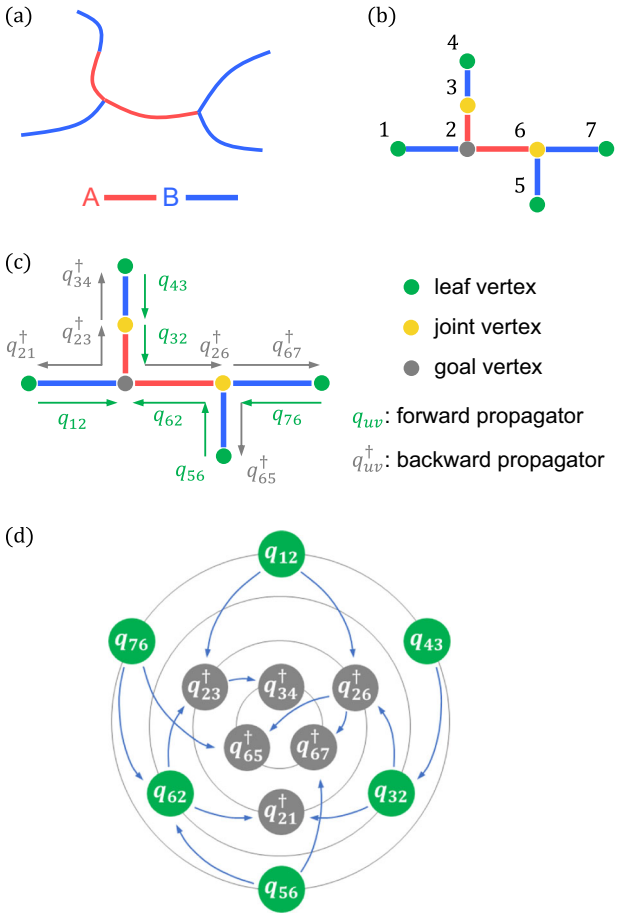

Fig. 1 | Schematic diagram of the graph representation of block copolymers. From a given block copolymer (**a**), we establish the graph representation and specify the types of vertices (**b**). **c** shows the allocation of propagators and **d** depicts the computation sequence of propagators.

edges for random generation and select appropriate range for f_A and χN values to enhance the possibility of hitting stability windows of the target phase. Detailed settings and the statistical analysis of the generated architectures can be found in Supplementary Note S5.

After screening over more than 6000 randomly generated architectures, we successfully identify two highly asymmetric miktoarm star block copolymers, denoted as $M_1 : A_1(B_1)_T(B_3)_TB_2A_2$ and $M_2 : A_1(B_3)_TB_2A_2$ as shown in Fig. 2, that exhibit notable stable windows for the PtS phase. This illustrates that our approach are able to stabilize another new phase in the well-explored AB-type block copolymer, without requiring custom-designed polymer architectures. In both architectures, the lengths of two A blocks are equal. We define the architectural parameters $\tau_{B_1} = f_{B_1}/f_B$ and $\tau_{B_2} = f_{B_2}/f_B$ being the ratio of the lengths of blocks B_1 and B_2 to the total length of all B blocks. Thus, M_2 can be considered as a special case of M_1 with $\tau_{B_1} = 0$, respectively. The phase diagram at the $\tau_{B_1} - \tau_{B_2}$ plane for fixed $f_A = 0.16, \chi N = 100$ is constructed as shown in Fig. 3. Density profiles of stable ordered phases predicted in this work are depicted in the right panel of Fig. 2. Free energy comparisons of various candidate phases along the transition path of changing τ_{B_2} with $\tau_{B_1} = 0.08$, and along the transition path of τ_{B_1} with $\tau_{B_2} = 0.20$, are presented in Supplementary Figs. S7 and S8.

The most remarkable feature exhibited in the phase diagram of Fig. 3 is the presence of two notable windows for PtS and iHP^a, occupying a band-shaped region from the upper-left portion to the lower-right portion. This band-shaped window separates the upper-right portion occupied by FCC and the lower-left portion occupied by several low-CN phases. Two common spherical phases BCC and HCP are found to be metastable. This result validates the effectiveness of the the random architecture strategy we employed, not only achieved the discovery of a new stable phase PtS but also obtained two architectures located inside and on the edge of the $\tau_{B_1} - \tau_{B_2}$ plane, respectively. It also suggests that the parameter we set for the number of blocks ($n_b = 5$) for generating architectures are reasonable for stabilizing low-CN phases.

Since f_A and χN are two important parameters in AB-type block copolymers, we further construct two phase diagrams at the $f_A - \chi N$ plane by fixing architectural parameters $\tau_{B_1} = 0.05, \tau_{B_2} = 0.25$ for molecule M_1 and $\tau_{B_1} = 0.00, \tau_{B_2} = 0.26$ for molecule M_2, as highlighted with blue dots in the phase diagram of Fig. 3. Molecule M_1 is located near the PtS − *FCC* FCC phase boundary, while molecule M_2 is located at the center of the stability window of PtS when $\tau_{B_1} = 0$. The phase diagrams of M_1 and M_2 are presented in the upper panel and lower panel of Fig. 4, respectively. The most remarkable feature shared by both phase diagrams is that the regions where BCC and close-packed spheres can usually be stabilized are mainly occupied by several low-*CN* CN phases including PtS and iHP^a. The stability window of PtS extends from the weak segregation region to the strong segregation region, and iHP^a remains the phase closest to PtS in terms of both the difference in free energy and the position of stable regions. In the phase diagram of M_1, FCC occupies a region near the phase boundary of PtS and iHP^a. While for M_2, stability windows of HEX, C_3, SC appear around the region of PtS. Cubic diamond (DS_C)[24], BCC and HCP are found to be metastable in both of the two phase diagrams. These predictions correspond to the positions of molecule M_1 and M_2 in the phase diagram of Fig. 3, respectively. Free energy comparisons of PtS and iHP^a along two transition paths in Fig. 4 can be found in Supplementary Fig. S9: one path involves changing f_A at $\chi N = 100.0$, and the other involves changing χN at $f_A = 0.15$.

For spherical phases with low coordination number, packing frustration is one of the most significant factors contributing to their difficulties in becoming stable phases. Typically, the Wigner-Seitz cell of such phases is polyhedral in shape, leading to uneven stretching of blocks forming the spherical domains to fill the space of the cell, resulting in entropy loss. To reduce uneven stretching, the polyhedral interfaces formed between species A and B can lead to an increase in interfacial energy. In order to address these conflicts, some artificially designed architectures distribute A-blocks on both sides of the molecule, with B-blocks acting as intermediary bridging blocks[23,24]. It can be observed that both of our molecules generated randomly satisfy this principle. The highly asymmetric B-blocks within the two A-blocks make it easier for the distantly located A domains to form, and the longer B_3 block ensure that there are sufficient segments to fill the broad gaps. Due to the branched nature of the two resulting molecules, the lengths of the B-blocks can be adjusted to separate them into different regions, thereby alleviating packing frustration. The shorter B_2 block acts as a bridge between separated spherical A-domains, with its degree of stretching adjustable by varying its proportion among all B-blocks. The distribution of the B_2 block is depicted in the density profile of PtS self-assembled by molecule M_2 (see Supplementary Fig. S10). By adjusting the volume fractions of B_2 and B_3, it is possible to simultaneously release packing frustration and construct bridging blocks, thereby stabilizing the target phase, PtS.

Discussion

It has been demonstrated that our proposed workflow, which begins with graph-enhanced SCFT, proceeds through massively parallel chain architecture screening, and ensures the reliability of free energy comparisons via the SAIS tool, can successfully discover new phases. Our highly customizable framework, for the first time, incorporates polymer architectures into the parameter space, offering a novel perspective on the search for new block copolymer self-assembly. Additional guiding principles can be identified using our method, enhancing the understanding of how polymer architectures regulate equilibrium morphologies. The capability to modify architectures in real-time further allows our framework to integrate existing metaheuristic algorithms, such as particle swarm optimization[44,45] and Bayesian optimization (BO)[46,47], to guide the inverse design of block copolymer architectures.

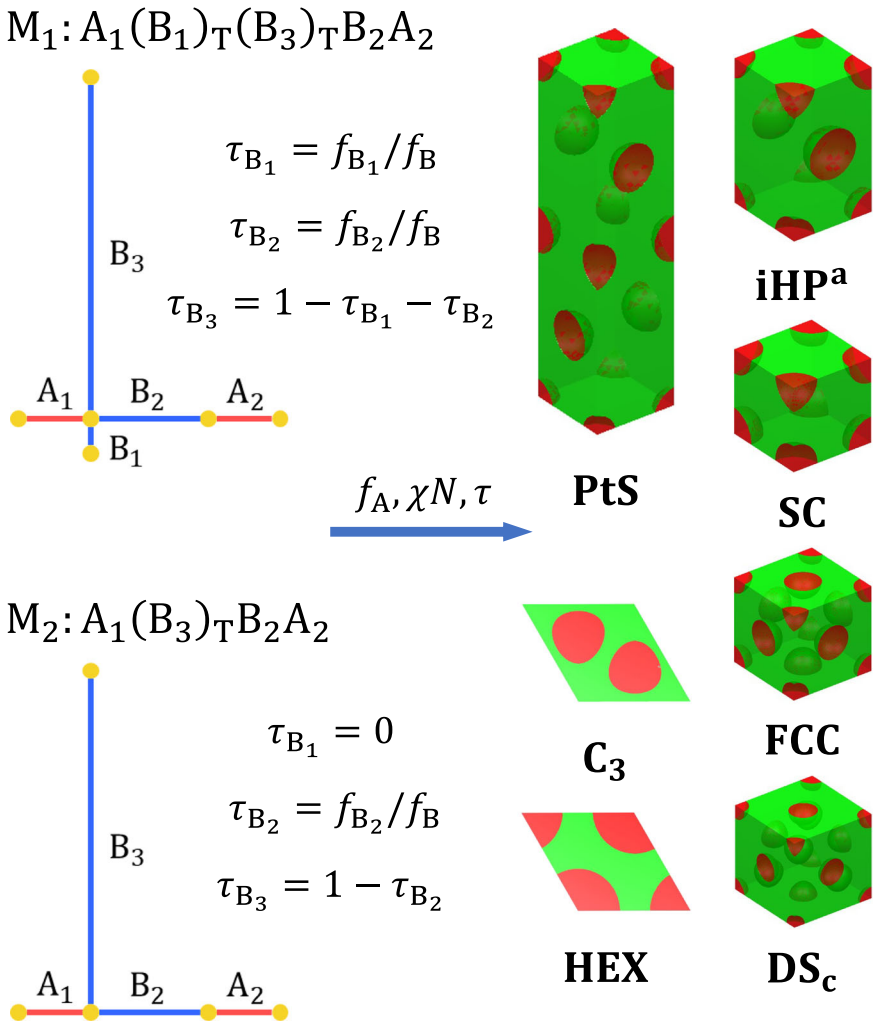

Fig. 2 | Schematic diagrams of the chain architectures and the primary candidate phases. Left panel: schematic for the two polymer architectures M_1 and M_2. Right panel: density profiles of typical ordered phases considered in this work including PtS, iHP[a], SC, FCC, DS_C, C_3, HEX.

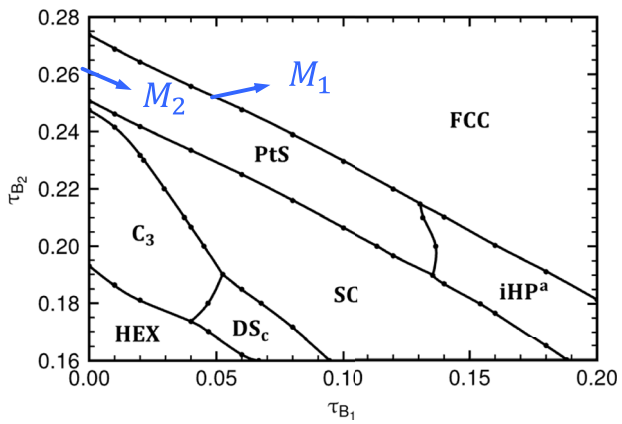

Fig. 3 | Phase diagrams. Phase diagram with respect to τ_{B_1} and τ_{B_2} for fixed $f_A = 0.16$, $\chi N = 100$. The two blue dots represent the positions of molecules M_1 and M_2 that we selected, respectively.

Our framework leverages well-established graph theory algorithms to represent and analyze chain architectures, which makes it easy to implement and adaptable to various polymer field theory simulations with negligible modifications. Various methods for MDEs, such as the spectral method[27,48], pseudospectral method[49,50], and the conventional finite difference methods[51,52], can all benefit from employing graph representation as the front-end for generic SCFT calculations. Furthermore, extension to multi-component systems is straightforward by applying this graph representation to each polymer component.

Beyond the screening for a given target phase, our workflow is also applicable to perform an exploration of indeterminate phases without any prior knowledge, thereby uncovering previously unknown ordered structures. It is based on the well-known fact that SCFT calculations can converge to either stable or metastable ordered phases locating at minima of the free energy surface[12]. Despite the stability window yet to be found, a variety of interesting morphologies have been discovered during the massive screening of architectures targeting phases such as PtS, TiO_2, Cu_2O, and SnI_4. Example novel phases include a $Cs_6[C_{60}]$ arrangement of spheres, a single continuous network in a cubic lattice and several morphologies featuring independent torus-shaped domains (see Supplementary Fig. S11).

It should be noted that the resulted chain architectures capable of stabilizing the target phase during a search without any restriction can be overly complicated. These architectures may manifest as linear chains tethered by copolymer blocks or as miktoarm molecules with inequivalent arms, rendering them challenging to prepare by conventional polymer synthesis techniques[53,54]. To increase the feasibility of resulted architectures, on one hand, we can restrict our exploration to a specific subset of architecture space by imposing conditions on the properties of blocks and joint vertices to avoid excessively intricate chain architectures. However, this approach may lead to failure in finding stability window for the target phase. On the other hand, recent experimental advancements[55–59] seems promising for precise control over each part of the chain architecture. Thus more and

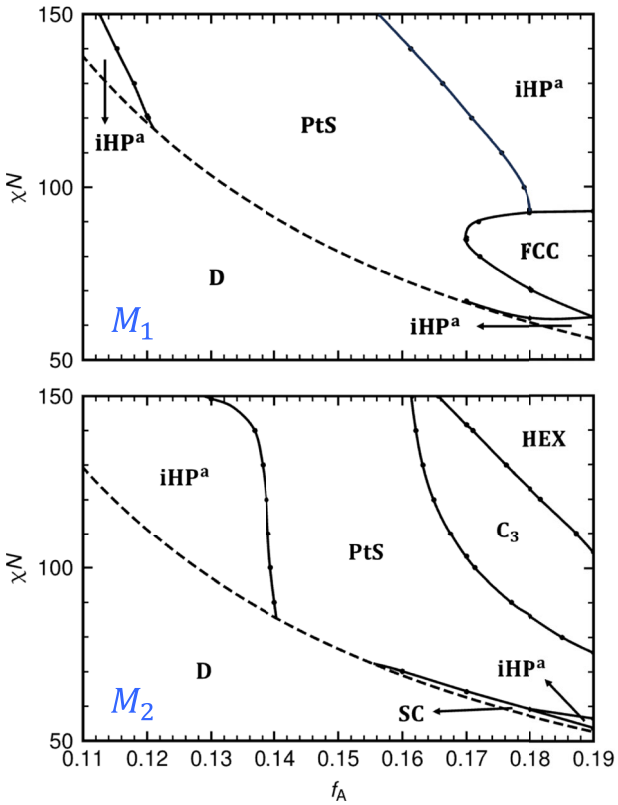

Fig. 4 | Phase diagrams. Phase diagrams of molecules M_1 (upper panel) and M_2 (lower panel). Dashed lines represent the approximate ODTs obtained by RPA theory, respectively.

more complicated architectures are expected to be feasible in the near future so that restrictions on the architecture searching space are no longer necessary.

In summary, we introduce a novel automated screening framework using graph-enhanced SCFT to explore the phase behavior of block copolymers, which allows for the unbiased discovery of new self-assembly. Our findings advance the research of block copolymer phase behavior, further enhancing our understanding of the extensively studied AB-type block copolymer. This approach is made possible by the graph-enhanced SCFT, which provides automated scheme for computing propagators and approximate ODTs. Supported by our pre-developed scattering-based identification tool, this workflow ensures reliable free energy comparisons for constructing phase diagrams. By performing a large number of parallel screening distributed randomly throughout the parameter space of interest, it becomes possible to repeatedly encounter stability windows of the target phase. Notably, the PtS phase is predicted as a new stable phase in AB-type block copolymers with two distinct architectures. Phase diagrams highlighting architectural parameters are constructed to describe their phase behavior around the PtS stability window. We believe this generic approach will become a valuable tool for stabilizing desired block copolymer self-assembly as well as exploring novel mesophases.

Methods

Graph representation

We developed the graph representation as a universal modeling approach for block copolymers. An undirected graph represents a block copolymer architecture, while a directed graph is used to analyze connectivity within the blocks. By utilizing depth-first search and topological sorting, any input architecture can be automatically analyzed to generate the necessary propagator sequence for computation. The graph representation offers a highly convenient interface for parameterizing block copolymer descriptions. Any non-cyclic block copolymer architecture can be automatically processed, whether input manually or randomly generated according to specified rules. This method is intended to enable the automatic generation of block copolymer architectures and subsequent SCFT computations without human intervention.

Self-consistent field theory (SCFT)

To compare the relative stability of candidate phases, we employ traditional SCFT as described in ref. 12. This involves calculating the free energies of all candidate phases for each polymer architecture under specific thermodynamic conditions. The stable phase is then identified based on the free energy minimization. We consider an incompressible polymer system composed of pure block copolymers and model each block as a Gaussian chain. Further details of the SCFT computation are provided in Supplementary Note S1.

Scattering-based automated identification strategy (SAIS)

This method is employed to ensure that each SCFT calculation converges to its initially specified phase without human supervision. As described in ref. 34, our pre-developed SIAS aims to identify the phase of a density distribution by computing its scattering features, including each possible Miller index and its corresponding scattering intensity (reflections and extinctions). A two-stage screening process is then used to compare the output with known ordered phases, ensuring that the computed mean-field free energy corresponds to the target structure, as SCFT initialized with a given structure may converge to other structures.

Random architecture exploration

To explore phase behavior within a more flexible search space and avoid potential limitations imposed by the a priori specification of a block copolymer architecture, we employ a random architecture strategy. Here, each architecture is formed by randomly combining a set of blocks, resulting in an ensemble of AB-type block copolymers encompassing tree-like, linear, and star architectures simultaneously. For each polymer architecture, the free energies of all candidate phases are obtained through automated SCFT calculations. The relative stability of the phases is then compared to identify the stable phase. Further details and parameters are provided in Supplementary Note S3.

Data availability

We provide a demo (https://github.com/DShKM118/PtS-demo) that includes detailed instructions for installing the Julia packages, constructing or randomly generating arbitrary chain architectures, and performing SCFT calculations for the PtS and iHP^a phases. This demo contains all the Julia packages needed to reproduce the results in our work.

Code availability

All the source code can be found in the demo. More details and functionalities of the Polyorder.jl pacakge can be found in the public documentation at: https://www.yxliu.group/Polyorder.jl/dev/.

Received: 30 September 2024; Accepted: 12 December 2024;
Published online: 18 December 2024

References

1. Braga, D. & Grepioni, F. *Crystal engineering: from molecules and crystals to materials* (Springer, 1999).
2. Glotzer, S. C. & Solomon, M. J. Anisotropy of building blocks and their assembly into complex structures. *Nat. Mater.* **6**, 557–562 (2007).
3. van Anders, G., Ahmed, N. K., Smith, R., Engel, M. & Glotzer, S. C. Entropically patchy particles: engineering valence through shape entropy. *ACS Nano* **8**, 931–940 (2014).
4. Dshemuchadse, J. Soft matter crystallography—complex, diverse, and new crystal structures in condensed materials on the mesoscale. *J. Appl. Phys.* **131** (2022).

5. Allmann, R. & Hinek, R. The introduction of structure types into the Inorganic Crystal Structure Database ICSD. *Acta Crystallogr. Sect. A* **63**, 412–417 (2007).
6. Lee, S., Bluemle, M. J. & Bates, F. S. Discovery of a frank-kasper σ phase in sphere-forming block copolymer melts. *Science* **330**, 349–353 (2010).
7. Hajduk, D. A. et al. A reevaluation of bicontinuous cubic phases in starblock copolymers. *Macromolecules* **28**, 2570–2573 (1995).
8. Grason, G. M., DiDonna, B. A. & Kamien, R. D. Geometric theory of diblock copolymer phases. *Phys. Rev. Lett.* **91**, 058304 (2003).
9. Grason, G. M. & Kamien, R. D. Interfaces in diblocks: a study of miktoarm star copolymers. *Macromolecules* **37**, 7371–7380 (2004).
10. Bates, F. S. & Fredrickson, G. H. Block copolymers–designer soft materials. *Phys. Today* **52**, 32–38 (1999).
11. Boles, M. A., Engel, M. & Talapin, D. V. Self-assembly of colloidal nanocrystals: From intricate structures to functional materials. *Chem. Rev.* **116**, 11220–11289 (2016).
12. Fredrickson, G. H. *The Equilibrium Theory of Inhomogeneous Polymers* (Oxford University Press, 2005).
13. Park, S. Y. et al. Dna-programmable nanoparticle crystallization. *Nature* **451**, 553–556 (2008).
14. Macfarlane, R. J. et al. Nanoparticle superlattice engineering with DNA. *Science* **334**, 204–208 (2011).
15. Li, Z. & Mao, C. Engineering colloidal crystals molecule by molecule. *Science* **384**, 741–742 (2024).
16. Wang, Y. et al. Synthetic strategies toward dna-coated colloids that crystallize. *J. Am. Chem. Soc.* **137**, 10760–10766 (2015).
17. Xie, N. et al. Macromolecular metallurgy of binary mesocrystals via designed multiblock terpolymers. *J. Am. Chem. Soc.* **136**, 2974–2977 (2014).
18. Matsen, M. W. Effect of architecture on the phase behavior of ab-type block copolymer melts. *Macromolecules* **45**, 2161–2165 (2012).
19. Xu, Z., Dong, Q. & Li, W. Architectural design of block copolymers. *Macromolecules* **57**, 1869–1884 (2024).
20. Matsen, M. W. Stabilizing new morphologies by blending homopolymer with block copolymer. *Phys. Rev. Lett.* **74**, 4225–4228 (1995).
21. Matsen, M. W. New fast scft algorithm applied to binary diblock copolymer/homopolymer blends. *Macromolecules* **36**, 9647–9657 (2003).
22. Xie, N., Li, W., Qiu, F. & Shi, A.-C. σ phase formed in conformationally asymmetric ab-type block copolymers. *ACS Macro Lett.* **3**, 906–910 (2014).
23. Tian, J., Deng, H., Li, W., Qiu, F. & Shi, A.-C. Formation of nonclassical ordered phases of ab-type multiarm block copolymers. *Phys. Rev. Lett.* **116**, 068304 (2016).
24. Xie, Q., Qiang, Y., Chen, L., Xia, Y. & Li, W. Synergistic effect of stretched bridging block and released packing frustration leads to exotic nanostructures. *ACS Macro Lett.* **9**, 980–984 (2020).
25. Xie, Q., Qiang, Y. & Li, W. Single gyroid self-assembled by linear babab pentablock copolymer. *ACS Macro Lett.* **11**, 205–209 (2022).
26. Matsen, M. W. & Bates, F. S. Block copolymer microstructures in the intermediate-segregation regime. *J. Chem. Phys.* **106**, 2436–2448 (1997).
27. Matsen, M. W. & Schick, M. Stable and unstable phases of a diblock copolymer melt. *Phys. Rev. Lett.* **72**, 2660–2663 (1994).
28. Matsen, M. W. & Schick, M. Stable and unstable phases of a linear multiblock copolymer melt. *Macromolecules* **27**, 7157–7163 (1994).
29. Matsen, M. W. & Bates, F. S. Unifying weak- and strong-segregation block copolymer theories. *Macromolecules* **29**, 1091–1098 (1996).
30. Hajduk, D. A. et al. Stability of the perforated layer (pl) phase in diblock copolymer melts. *Macromolecules* **30**, 3788–3795 (1997).
31. Tyler, C. A. & Morse, D. C. Orthorhombic *fddd* network in triblock and diblock copolymer melts. *Phys. Rev. Lett.* **94**, 208302 (2005).
32. Tang, C., Lennon, E. M., Fredrickson, G. H., Kramer, E. J. & Hawker, C. J. Evolution of block copolymer lithography to highly ordered square arrays. *Science* **322**, 429–432 (2008).
33. Xu, W., Jiang, K., Zhang, P. & Shi, A.-C. A strategy to explore stable and metastable ordered phases of block copolymers. *J. Phys. Chem. B* **117**, 5296–5305 (2013).
34. Zhang, Y.-C., Huang, W.-L. & Liu, Y.-X. Automated identification of ordered phases for simulation studies of block copolymers. *Chin. J. Polymer Sci.* **42**, 683–392 (2024).
35. Rozhdestvina, V., Udovenko, A., Rubanov, S. & Mudrovskaya, N. Structural investigation of cooperite (pts) crystals. *Crystallogr. Rep.* **61**, 193–202 (2016).
36. Yang, Y. Graph theory of viscoelastic and configurational properties of gaussian chains. *Macromol. Theory Simul.* **7**, 521–549 (1998).
37. Reyes, M. L. P., Reyes, G. E. & Zolfaghari, H. *Generic figures and their glueings: A constructive approach to functor categories* (Polimetrica, 2004).
38. Even, S. *Graph Algorithms* (Cambridge University Press, 2011).
39. Cormen, T. H., Leiserson, C. E., Rivest, R. L. & Stein, C. *Introduction to algorithms* (MIT Press, 2009).
40. Leibler, L. Theory of microphase separation in block copolymers. *Macromolecules* **13**, 1602–1617 (1980).
41. Ranjan, A., Qin, J. & Morse, D. C. Linear response and stability of ordered phases of block copolymer melts. *Macromolecules* **41**, 942–954 (2008).
42. Shi, W. Scattering function and spinodal transition of linear and nonlinear block copolymers based on a unified molecular model. *Chin. J. Polym. Sci.* **39**, 779–788 (2021).
43. Russel, S. & Norvig, P. *Artificial intelligence: a Modern approach* (Prentice Hall, 2021),.
44. Khadilkar, M. R., Paradiso, S., Delaney, K. T. & Fredrickson, G. H. Inverse design of bulk morphologies in multiblock polymers using particle swarm optimization. *Macromolecules* **50**, 6702–6709 (2017).
45. Case, L. J., Delaney, K. T., Fredrickson, G. H., Bates, F. S. & Dorfman, K. D. Open-source platform for block polymer formulation design using particle swarm optimization. *Eur. Phys. J. E* **44**, 115 (2021).
46. Garnett, R. *Bayesian optimization* (Cambridge University Press, 2023).
47. Dong, Q. et al. Inverse design of complex block copolymers for exotic self-assembled structures based on bayesian optimization. *ACS Macro Lett.* **12**, 401–407 (2023).
48. Matsen, M. W. Fast and accurate scft calculations for periodic block-copolymer morphologies using the spectral method with anderson mixing. *Eur. Phys. J. E* **30**, 361 (2009).
49. Tzeremes, G., Rasmussen, K. O., Lookman, T. & Saxena, A. Efficient computation of the structural phase behavior of block copolymers. *Phys. Rev. E* **65**, 041806 (2002).
50. Rasmussen, K. & Kalosakas, G. Improved numerical algorithm for exploring block copolymer mesophases. *J. Polym. Sci. Part B* **40**, 1777–1783 (2002).
51. Drolet, F. & Fredrickson, G. H. Combinatorial screening of complex block copolymer assembly with self-consistent field theory. *Phys. Rev. Lett.* **83**, 4317–4320 (1999).
52. Drolet, F. & Fredrickson, G. H. Optimizing chain bridging in complex block copolymers. *Macromolecules* **34**, 5317–5324 (2001).
53. Dau, H. et al. Linear block copolymer synthesis. *Chem. Rev.* **122**, 14471–14553 (2022).
54. Bates, M. W. et al. Synthesis and self-assembly of abn miktoarm star polymers. *ACS Macro Lett.* **9**, 396–403 (2020).
55. Woo, D. et al. High-density packing of spherical microdomains from a(ab3)3 dendron-like miktoarm star copolymer. *ACS Macro Lett.* **13**, 8–13 (2024).
56. Hou, W. et al. Rapid and efficient synthesis of star polymers via arm-first monomer emulsified aqueous ring-opening metathesis polymerization (me-romp). *Macromolecules* **57**, 3173–3182 (2024).

57. Ma, Z. et al. Discrete miktoarm star block copolymers with tailored molecular architecture. *ACS Polym. Au* **3**, 457–465 (2023).
58. Seo, Y., Woo, D., Li, L., Li, W. & Kim, J. K. Phase behavior of ps-(ps-b-p2vp) miktoarm star copolymer. *Macromolecules* **54**, 7822–7829 (2021).
59. Levi, A. E. et al. Efficient synthesis of asymmetric miktoarm star polymers. *Macromolecules* **53**, 702–710 (2020).

Acknowledgements

We are grateful to Glenn H. Fredrickson for thoughtful discussions and valuable comments on this work. This research was supported by the National Natural Science Foundation of China (Grants No. 21873021).

Author contributions

Yi-Xin Liu conceived and supervised this work. Yuchen Zhang designed and performed the simulations. Weiling Huang provided support with data analysis and interpretation. All authors discussed the results and contributed to the writing of the manuscript.

Competing interests

The authors declare no competing interests.

Additional information

Supplementary information The online version contains supplementary material available at https://doi.org/10.1038/s43246-024-00723-w.

Correspondence and requests for materials should be addressed to Yi-Xin Liu.

Peer review information *Communications materials* thanks George Kalosakas and the other, anonymous, reviewer(s) for their contribution to the peer review of this work. Primary Handling Editors: Jack Evans and Jet-Sing Lee. A peer review file is available.